Dispersion of Cellulose Crystallites by Nonionic Surfactants in a Hydrophobic Polymer Matrix

Jooyoun Kim,[1] Gerardo Montero,[1] Youssef Habibi,[1] Juan P. Hinestroza,[2] Jan Genzer,[3] Dimitris S. Argyropoulos,[1] Orlando J. Rojas[1]

[1] *Forest Biomaterials Science and Engineering, North Carolina State University, Raleigh, North Carolina 27695-8005*

[2] *Fiber Science Program, Cornell University, Ithaca, New York 14853*

[3] *Chemical and Bimolecular Engineering, North Carolina State University, Raleigh, North Carolina 27695-7905*

Cellulose nanoparticles obtained by acid hydrolysis of cellulose paper were used to reinforce polystyrene composite films. The nonionic surfactant sorbitan monostearate was utilized to improve the dispersion properties of the hydrophilic cellulose in hydrophobic matrix and to prevent the formation of aggregates. Turbidity tests were used to measure dispersion stability of the cellulose crystallites in the hydrophobic solvent used in the composite manufacture. A correlation was found between the dispersion stability in solvent and the formation of aggregates in the polymeric composites. Nanocomposite films were processed using a casting/evaporation technique. Thermal and mechanical properties of processed composites were studied by differential scanning calorimetry (DSC) and dynamical mechanical analyses (DMA), respectively. The results showed that the optimum addition of surfactant produced better dispersion of the cellulose particles in the polystyrene matrix and improved the mechanical properties of the resulting composite due to an enhanced compatibility. POLYM. ENG. SCI., 49:2054–2061, 2009. © 2009 Society of Plastics Engineers

INTRODUCTION

Cellulose-based microstructures offer unique opportunities due to their high stiffness/strength, hydrophilicity, biocompatibility, stereoregularity, biodegradability, chemical stability, and ability to form superstructures. Furthermore, the ease of surface chemical modification makes cellulose a suitable candidate for use in composites. Depending on their origin, cellulose (nano)fibrils possess diameters ranging from 3 to 20 nm with a high aspect ratios [1–3]. Several uses have been identified for such fibrils including reinforcing composite materials [4–8], non-caloric thickening agents in food products [9], edible coatings [10], drug delivery agents [11], etc. Current interests in the development of sustainable bio-based products have been triggered by the emerging shortage of petrochemical raw materials. To this end, this work is aimed at exploring the utilization of biomass products in the manufacturing of composite materials combining synthetic and natural components.

A homogeneous dispersion of cellulose particles in a polymeric matrix is required for obtaining well-defined mechanical properties and consistent performance of the final composite material. Aggregation of the dispersed phase has a detrimental impact resulting in undesirable effects on the final composite as aggregates act as stress concentrators [12, 13].

Preventing the presence of aggregation effects is not a trivial issue, for example when dispersing (hydrophilic) cellulose particles in hydrophobic matrices. This is mainly due to the lack of compatibility between the two phases. Therefore, in order to prevent the cellulose from aggregating and to improve its dispersion in the matrix material, modification of cellulose surfaces is required.

Some of the cellulose surface modification techniques include graft polymerization [12, 14, 15], silylation of —OH groups in the polymer [16–20], and the use of surfactants [12, 21–23]. Among these options, the use of surfactant as dispersant is of interest due to its simplicity. In this latter case, it is proposed that the hydrophilic head group of the surfactant adsorbs on the cellulose fibril surface whereas its hydrophobic tail finds proper solvency conditions in the matrix, thus deterring aggregation of the cellulose inclusions via steric stabilization [24].

Correspondence to: Prof. Orlando J. Rojas; e-mail: ojrojas@ncsu.edu
Contract grant sponsor: NCSU Nanotechnology Steering Committee; contract grant sponsor: National Research Initiative of the USDA Cooperative State Research, Education and Extension Service; contract grant number: 2007-35504-18290; contract grant sponsor: National Science Foundation Materials Research Science and Engineering Centers (MRSEC) program; contract grant number: DMR 0520404.
DOI 10.1002/pen.21417
Published online in Wiley InterScience (www.interscience.wiley.com).

The chief goal of this study involved the isolation of cellulose nanofibril aggregates (called thereafter cellulose nanoparticles, CN) and their use to reinforce a hydrophobic polymer matrix (polystyrene, PS). In order to improve the adhesion of cellulose fibrils to the surrounding matrix, a non-ionic surfactant, a sorbitan monostearate, was used to stabilize the dispersed phase. The dispersion stability of CN in the precursor hydrophobic solvent was measured via turbidity and the results were used to account for their aggregation behavior in the solid PS composite films. The composite films were characterized using optical imaging and atomic force microscopy (AFM), differential scanning calorimetry (DSC), and dynamic mechanical analysis (DMA). The knowledge gained from this work will allow for tailoring the functionalities and properties of the resulting composites based on the chemical nature of the reinforcing particles as well as the compatibility of the dispersing agent.

EXPERIMENTAL

Materials

Polystyrene (Mw 230,000), Whatman® No.1 cellulose filter paper, hydrochloric acid (HCl) and sorbitan monostearate (Span-60) were purchased from Sigma-Aldrich (St. Louis, MO). Tetrahydrofuran (THF) was obtained from B&J Brand™ (Muskegon, MI).

Preparation of Cellulose Nanoparticles

Cellulose nanoparticles (CN) were prepared by HCl-assisted hydrolysis of Whatman® cellulose filter paper. Typically, 20 g of filter paper were dispersed using Osterizer blender in 700 mL aqueous 1.5 M HCl solution after which cellulose hydrolysis was allowed during 4 hr at 100°C. After the hydrolysis, the suspension was diluted using deionized water and centrifuged several times at 2,800 rpm to remove acid from the cellulose dispersion (until neutral pH). Fine CNs were re-suspended in water after the last 2,800 rpm centrifuge cycle and were then collected and subjected to additional centrifugation at higher speeds: Centrifugation at 8,000 rpm for 30 min followed by centrifugation at 14,000 rpm for additional 30 min (using an Automatic Servall® Superspeed Centrifuge) was performed to obtain a well defined particle size distribution. The cellulose nanoparticles that were separated after high speed centrifugation were collected and dried using freeze dry/shell freeze system (Labconco, Kansas City, MU). These nanoparticles were used in the creation of composite films as explained later in this section.

AFM Characterization of Cellulose Nanoparticles

A few drops of solution of the cellulose nanoparticles dispersed in water were placed onto a silica wafer which was previously immersed in a 100 mg/l aqueous solution of polyvinyl amine for 20 min and subsequently dried. Polyvinyl amine was used as an anchoring polymer to improve the adhesion of CN to the silica substrate. A Q-Scope 350 AFM (Quesant Instruments Co., Santa Cruz, CA) was used to image the CN. NSC16 cantilevers (Quesant Instruments Co.), with resonance frequency of 170 ± 20 and a spring constant of 42.5 ± 17.5 were used for intermittent contact mode AFM operation.

Preparation of Composite Films

Composite films were prepared by solvent-casting using polystyrene (PS) as the matrix polymer and cellulose nanoparticles (CN) as reinforcing material. CNs were dispersed in THF under ultrasonication for few minutes, and a fixed amount of the surfactant was added while stirring until complete homogenization. Finally, the respective volume of 10% (w/w) solution of PS in THF was added and the suspension was stirred overnight to ensure good dispersion. The dispersion was then cast into Fisher brand® aluminum weighing dishes (Fisher Scientific, Pittsburgh, PA). After THF evaporation at ambient conditions the films coated uniformly the bottom of the aluminum dish. The relative weight ratios of PS to CN were varied from 97:3 to 94:6. We used comparatively low amounts of CN because higher load of unmodified cellulose in hydrophobic matrices is extremely difficult to process. We note that in the case of water soluble and hydrophilic polymer matrices much higher addition levels of the dispersed phase are possible.

In order to investigate the effect of CN stabilization in the manufacture of the composite films the non-ionic surfactant was used at different concentrations (CN: Surfactant ratios of 1:0 (no surfactant), 1:1, 1:2, and 1:4). These CN : Surfactant ratios were selected after estimation of available surface area in the CNs and optimized from preliminary experiments using turbidity measurements. It is worth noting that the relative amount of PS and CN in all composites tested was fixed so that we were able to unveil the contribution of the surfactant. The resulting composite films were imaged using an optical microscope (Olympus BH2-UMA, Japan) equipped with a video camera (Sony® DXC-970 MD) at 100X magnification.

Turbidity Measurements

The turbidity of dispersions of CN in THF precursor solvent was monitored in order to establish a correlation between CN stability and mechanical properties of the resulting CN/PS composites. A DRT-15CE Turbidimeter (HF Scientific, Inc., Fort Myers, FL) was used to measure the turbidity using a linear scale throughout ranges in Nephelometric Turbidity Units (NTU). At least three measurements were obtained for each sample but only the average values are presented thereafter. We note that the coefficient of variation was less than 0.17 for all the

experimental measurements. A low turbidity of the dispersion was taken as indicative of a large amount of CN particles settled due to precipitation of aggregates. On the other hand, better dispersions of CN in THF were expected to exhibit higher turbidities. In a turbidity test 20 ml of CN dispersed in THF (0.3 and 0.6 wt%) were used after 24 h stirring. Note that these concentrations of CN corresponded to the amount used in CN-loaded PS composite films (3 and 6 wt% of CN) prepared with 10 wt% solution in THF. Surfactant was added to the respective dispersions and specified as weight ratio with respect to CN, i.e., CN:Surfactant of 1:1, 1:2, and 1:4.

Differential Scanning Calorimetry

Differential Scanning Calorimetry (DSC Q200 from TA Instruments) measurements were conducted in order to examine the effect of surfactant on the thermal properties (and particularly the glass transition temperature, T_g) of the composite films. Around 10 mg of samples were placed in a DSC cell in glove box. Each sample was heated from 25 to 150°C at a heating rate of 10°C/min. The glass transition temperature T_g was taken as the inflection point of the specific heat increment at the glass-rubber transition.

Dynamic Mechanical Analysis

A TA 2980 Dynamic Mechanical Analyzer (DMA) was used to probe the mechanical properties of the composite films under tension as a function of temperature. All the measurements were carried out at a constant frequency of 1 Hz, strain amplitude of 0.07%, a temperature range of 100–200°C, a heating rate of 3°C/min and gap distance of 10 mm. The samples were prepared by cutting strips from the films with dimensions 20 × 5 × 0.3 mm. DMA tests were carried out in duplicate with an observed experimental error of about ±3%.

RESULTS AND DISCUSSION

Isolation of Cellulose Nanoparticles

Cellulose nanoparticles (CNs) were obtained via the hydrolysis of Whatman® cellulose filter paper. The amorphous phase at the interface of microcrystalline domains in these fibers (along the microfibril length) was removed by acid treatment to produce the cellulose nanoparticles. Such cellulosic materials possess high mechanical modulus and therefore are excellent candidates for the manufacture of composite materials. The length (measured by AFM) of CN nanoparticles was in the 200–500 nm range while the width between 10 to 20 nm (Fig. 1). However, aggregated crystals were observed.

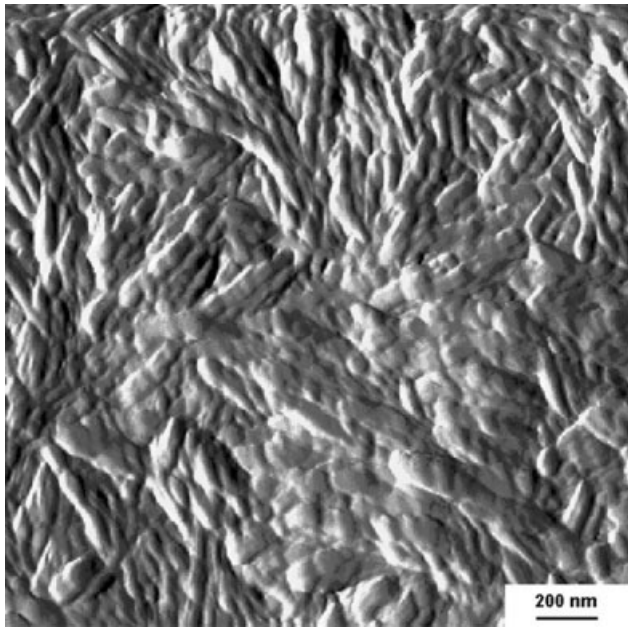

FIG. 1. AFM tapping mode image of cellulose nanoparticles obtained by acid hydrolysis of filter paper.

Composite Films With PS Matrix and Cellulose Reinforcing Particles

The use of abundant, readily available cellulose as the dispersed phase in composites is expected to be beneficial because cellulose has a high elastic modulus. Therefore, addition of cellulose nanoparticles can improve the mechanical properties of the resulting composites while enhancing their absorption and biodegradation characteristics.

Before composites processing we studied the dispersion and the stability of CNs in the casting solvent. In fact, we hypothesize that the dispersion stability of CN in the final composites could be predicted by evaluating the dispersion properties of cellulose in the casting solvent before the polymeric component (PS) was added. Higher dispersion stability of CN within the hydrophobic solvent may lead to better dispersion of cellulose within the hydrophobic polymer matrix. The dispersion stability, on the other hand, can be easily determined from turbidity measurements of the cellulose dispersions. As the cellulose nanoparticles aggregate and settle down the dispersion becomes less turbid. Lipophilic sorbitan monostearate surfactant (HLB 4.7) was used as a dispersing agent to improve the stabilization of the cellulose in the organic solvent. Figure 2 illustrates the reduction of turbidity with time of 0.3 and 0.6 wt% CN dispersions in THF. Note that if 10 wt% of PS solution is added to the THF dispersions containing 0.3 or 0.6 wt% CN, a PS-CN composite with 3 or 6 wt% of cellulose crystallites would be obtained, respectively.

Figure 2A shows the case of a dispersion of 0.3 wt% CN without surfactant that has settled down relatively quick compared to the dispersions containing surfactant.

 DOI 10.1002/pen

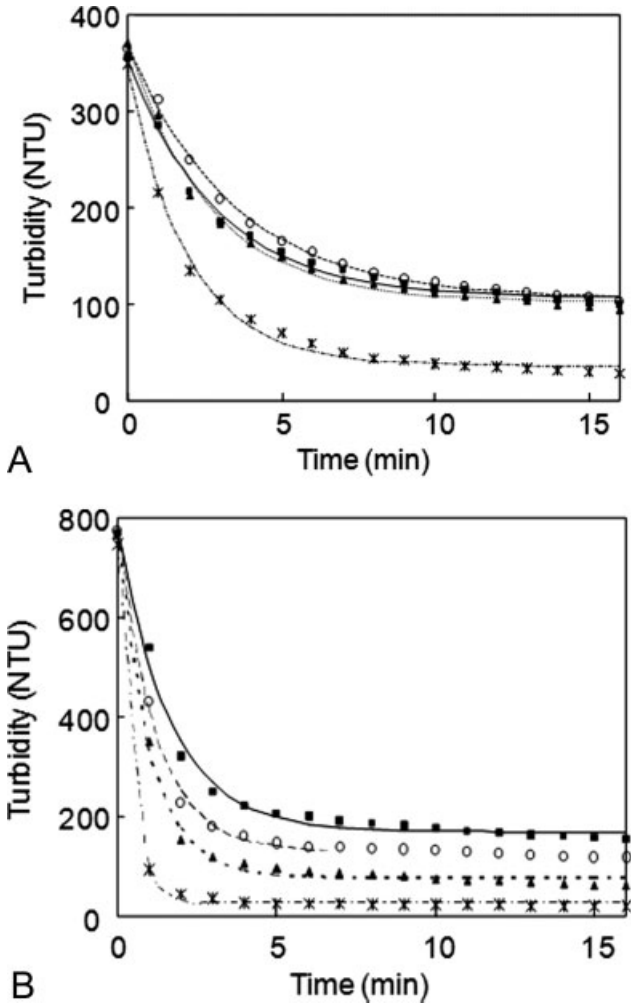

FIG. 2. Turbidity measurements of CN in THF for 0.03 wt% of CN in THF (A) and 0.06 wt% of CN in THF (B). The respective surfactant concentrations are indicated by the following symbols: * CN:Surfactant = 1:0, ■ CN:Surfactant = 1:1, ○ CN:Surfactant = 1:2, ▲ CN:Surfactant = 1:4. The added lines were fitted to the experimental data according to $\tau = A \times \exp(Bt + C)$.

It can be seen that the dispersion stability at CN:Surfactant ratio of 1:2 was the highest.

For 0.6 wt% CN dispersion in THF, a considerable difference in its turbidity was noted when surfactant was added. A 0.6 wt% of cellulose dispersion without surfactant exhibited the lowest dispersion stability or turbidity. A 1:1 ratio of CN:Surfactant showed the highest initial turbidity values. As more surfactant was added to the dispersion, its stability decreased, probably due to self-aggregation of the nonionic surfactant in the form of micellar structures. As the surfactant concentration is increased further the effect of the surfactant becomes deleterious to the stability of the dispersions.

The evolution of turbidity (τ) as a function of settling time can be fitted a simple exponential decay equation as follows:

$$\tau = A \times \exp(Bt + C) \quad (1)$$

where τ is the turbidity (NTU), t the time (seconds) and A, B and C are constants for the best fit of the experimental data.

Table 1 lists the exponential constants obtained from the best-fit of the turbidity, the initial turbidity decay rate $(d\tau/dt)_{t=0}$, difference between the initial turbidity (τ_i) and that recorded after 16 min (τ_f), and the time needed to achieve half the original turbidity value ($t_{\tau_{i/2}}$). The aforementioned parameters are useful in judging the dispersion stability because they can be utilized to determine the desired dispersion properties of the material. For example, in order to predict the dispersion stability and aggregation in the produced composite films, the final turbidity value or $\tau_i - \tau_f$ may be important consideration for systems with low solvent evaporation rates. For the systems where the initial dispersion stability is more important, the initial turbidity decay rate, $(d\tau/dt)_{t=0}$, may be a more relevant consideration.

The turbidly data, as discussed before, were compared with the direct observation of the homogeneity of cellulose dispersion in THF and that of the cellulose nanoparticles within the resulting composites. Faster deterioration of cellulose dispersion stability, $(d\tau/dt)_{t=0}$, is attributed to additional cellulose aggregation within the composite film, while slower turbidity decay is found to be related to a reduced tendency for coalescence and aggregation.

From the turbidity measurements performed with 0.3 and 0.6 wt% cellulose dispersions, it appears that it is the surfactant concentration in the solvent rather than the ratio of cellulose to surfactant that affects the stability of the dispersion.

TABLE 1. Prefactor (A), time (B), and exponential (C) constants for turbidity of 0.3 and 0.6% CN in THF dispersions.

% of CN	0.3% CN				0.6% CN			
CN:Surfactant	1:0	1:1	1:2	1:4	1:0	1:1	1:2	1:4
A	307	246	263	267	723	607	649	695
B	−0.51	−0.35	−0.29	−0.37	−2.31	−0.60	−0.83	−0.97
C	36.8	107	106	103	25.7	170	129	76.8
$(d\tau/dt)_{t=0}$	−155	−84.9	−77.2	−100	−1670	−366	−540	−670
$\tau_i - \tau_f$ [NTU]	320	256	263	275	728	611	657	707
$t_{\tau_{i/2}}$ [min]	1.62	3.66	4.13	3.15	0.32	1.69	1.10	0.84

A, B, C are constants for the best fit of experimental values to $\tau = A \times \exp(Bt + C)$.

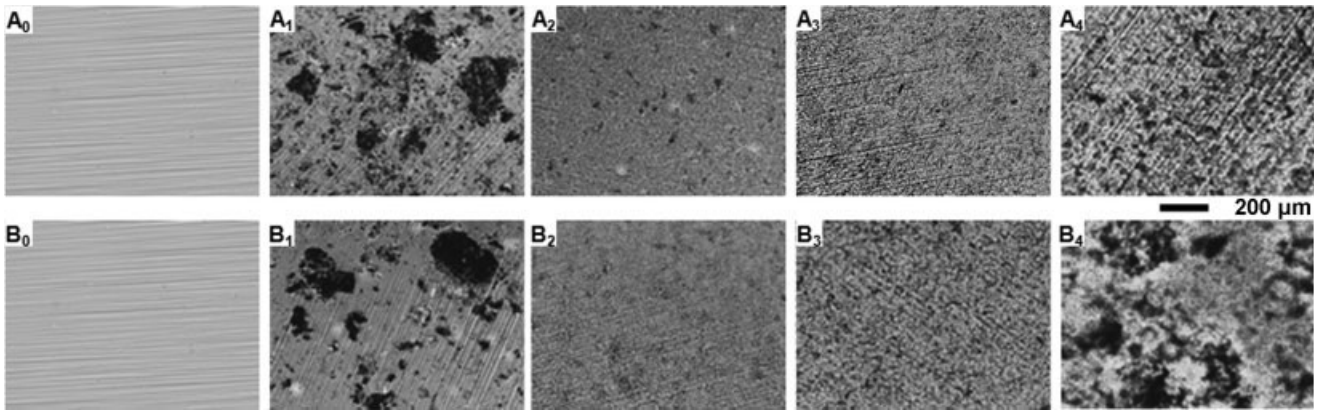

FIG. 3. Optical microscope images for neat PS film (A_0 and B_0) and PS/CN/Surfactant composite films with 3% (A_{1-4}) and 6% (B_{1-4}) CN weight load. CN:Surfactant ratios are 1, CN:Surfactant = 1:0; 2, CN:Surfactant = 1:1; 3, CN:Surfactant = 1:2; 4, CN:Surfactant = 1:4.

For all experiments performed using 0.6 wt% of CN, the solution containing a CN:Surfactant ratio of 1:1 showed the greatest dispersion stability. However, for the experiments carried out using 0.3 wt% of CN in the dispersion, the formulation having a CN:Surfactant ratio of 1:2 exhibited the best stability characteristics. For both cases, the concentration of surfactant was 0.6 wt% in THF.

The PS/CNs composites were processed by casting-evaporation technique with different amounts of CNs and with nonionic surfactant added at different ratios. The morphology of the films was monitored by optical microscopy. An image of a PS film without CNs is shown in Fig. $3A_0$ and B_0. Note that the streaks in the figure result from the pattern present on the aluminum dish used as a casting substrate. As reported elsewhere [12, 13], the stability of the dispersed phase in a polymer matrix constitutes a challenge, especially when the dispersed phase and the matrix have different hydrophilicity and surface energy. As illustrated in Fig. $3A_1$, adding 3 wt% of cellulose to a PS matrix resulted in aggregation of cellulose nanoparticles.

As explained before, nonionic surfactant was used as a dispersing agent to improve the stabilization of the cellulose crystallites within the PS matrix. When the same weight ratio of surfactant to cellulose was used (surfactant was 3 wt % of PS matrix, or 0.3 wt% of THF solution), a decrease in the degree of aggregation was observed (Fig. $3A_2$). Further an increase in the concentration of surfactant up to 0.6 wt% in THF solution appeared to improve the dispersion of the CNs (Fig. $3A_3$). However, increasing surfactant concentration further, up to 1.2 wt% in THF solution (1:4 ratio of CN to surfactant) resulted in agglomeration. This could be explained by the effect of self-aggregation of the surfactant, which becomes a factor in the destabilization of the cellulose nanoparticles.

Similar trends in the aggregative behavior were displayed for systems with 6 wt% of cellulose CNs in PS matrices (Fig. $3B_1$). The optimum dispersion appears at CN:Surfactant ratio of 1:1, where the concentration of surfactant in THF solution is about 0.6 wt%. At higher surfactant concentration, more aggregation of cellulose was observed.

Differential Scanning Calorimetry (DSC) analysis revealed the effect of CN and surfactant addition on the T_g of the respective composite films. The films were examined over a temperature range of 25–150°C (thus decomposition and evaporation of surfactant was prevented). The melting point Tm of the nonionic surfactant was found to be 53–54°C as was clearly observed in the DSC peaks of films in the presence of increased amounts of the surfactant (see Fig. 4).

The T_g of the composite films was found to depend on the concentration of surfactant. For cast films without surfactant the T_g was determined at about 93°C; which is also the T_g value for neat polystyrene matrix. Similar behavior was reported in other studies; surprisingly the addition of cellulose nanocrystals in the polymers matrices did not to affect appreciably the glass-rubber transition temperature

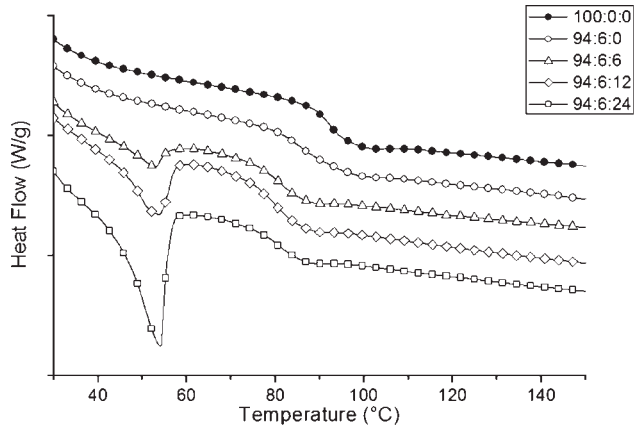

FIG. 4. DSC analysis for neat PS and 6% CN PS/CN composite films and different surfactant concentrations. The inset shows the relative ratios X:Y:Z where X is the % PS, Y is the % CN (w/w) with respect to PS and Z is the surfactant concentration, also as weight % with respect to PS mass.

 DOI 10.1002/pen

T_g values, regardless of the nature of the host polymer, the origin of the CNs or the processing conditions [25]. This observation is unexpected if one considers the nature and high specific area of CNs.

When the amount of surfactant added to the formulation increased, the T_g of the film was reduced significantly until it reached a constant value of 80°C; this change is related to the change in molecular motion of the polymer matrix at the interface between the matrix and the filler and the plasticizacing effect of the added surfactant. Similar effect was showed for nanocomposites loaded with moisture-sensitive cellulose whiskers [26], this was related to the plasticization effect of water and also linked to the strong interaction between CNs and the matrices. The plasticizing effect of glycerol [27] or sorbitol [28] in starch reinforced with cellulose whiskers was also reported to be the origin of changes in T_g.

Dynamic Mechanical Analysis

Dynamic Mechanical Analyzer (DMA) tests were performed on the cast films of neat PS and PS-based nanocomposites reinforced with cellulose nanoparticles, with and without surfactant added. At the onset of our discussion we note that we observed an increase in the mechanical properties of the composites with respect to the neat polymer matrix. However, the observed increase in the mechanical properties is modest if it is compared with other nanocomposites with cellulose. This observation is explained by the fact that the polystyrene matrix is in itself very strong and therefore the contribution from the reinforcing cellulose nanocrystals is easily screened.

Figure 5 shows the normalized curves of the storage modulus (E′) as a function of temperature for the different composites. As it is well-known, the exact determination of the glassy modulus depends on the precise dimensions of the sample. To avoid this effect, normalization of the curves can be carried out, especially when no significant difference are observed in the raw curves at the glassy modulus.

The unfilled matrix (Fig. 5A) displayed the typical behavior of an amorphous thermoplastic polymer. For temperatures below T_g the polymer was in the glassy state and the modulus remained roughly constant around 2.72 GPa. The onset of the (distinctive) drop in the storage modulus, corresponding to the glass rubber transition, was observed at 90°C. This modulus drop is therefore ascribed to an energy dissipation phenomenon involving cooperative motions of the polymer chain; DMA measurement failed at above 125°C because of chain disentanglement effects which are common in amorphous polymers.

With addition of cellulose nanoparticles (3 and 6%, Fig. 5A), similar behavior of storage modulus E′ with temperature was observed. However, the softening temperature decreased monotonically with the addition of the CNs as can be illustrated by the softening points of 82 and 77°C for the composites containing 3 and 6% of CN,

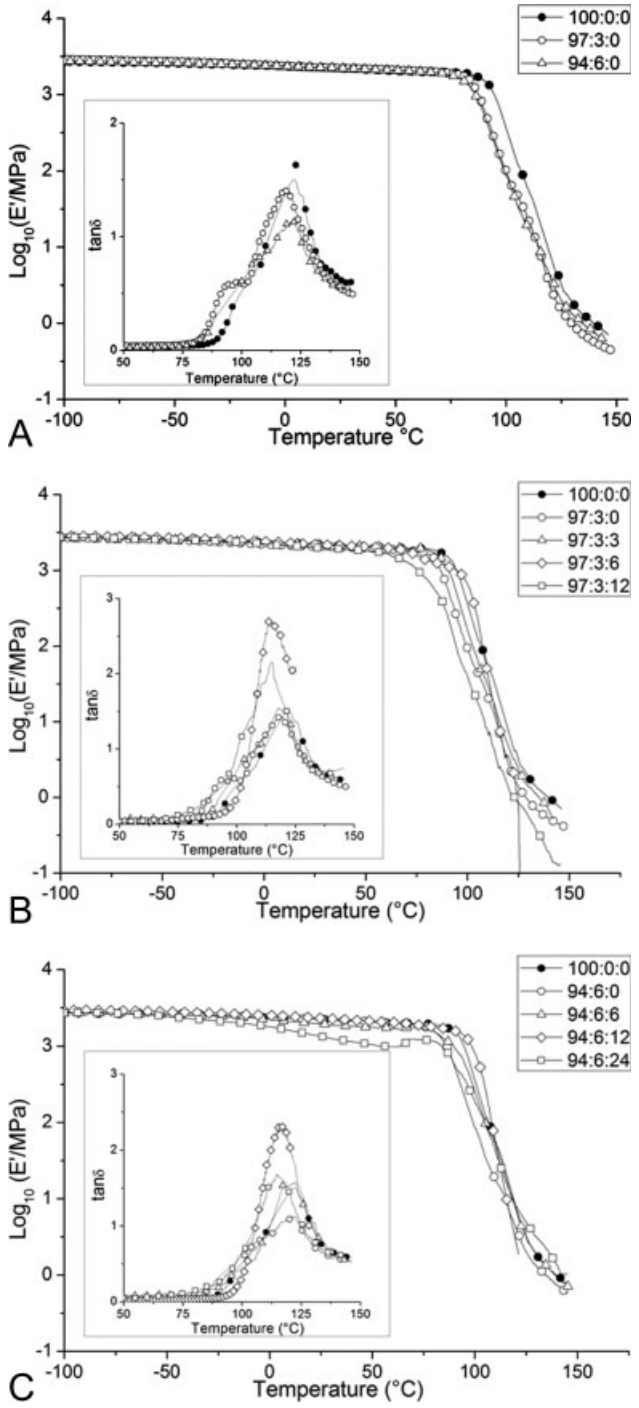

FIG. 5. Logarithm of the storage tensile modulus E′ and tan δ (inset) versus temperature at 1 Hz for PS nanocomposites reinforced with different contents of cellulose nanoparticles, CNs. The ratio PS:CN:Surfactant for the different composites tested are shown in the respective legends.

respectively. This decrease in the thermal stability is probably a consequence of poor dispersion of CNs and/or formation of CN aggregates. When surfactant was added to the composite containing 3 and 6% of CNs (Fig. 5B and C), the storage modulus displayed similar behavior as that explained above but the storage softening temperature

shifted up as the weight ratio CN:Surfactant was increased from 1:1 or 1:2. When an excess of surfactant was added to the composites, the storage modulus dropped in the glassy region which corresponds to the melting of the surfactant. In addition, the storage softening temperature drop shifts down, probably due to the plastizising effect brought about excess surfactant.

The evolution of the tangent of the loss angle (tan δ) was studied as a function of temperature for all composites, as illustrated in the insets of Fig. 5. The observed relaxation phenomenon is associated with the glass transition of the polymeric matrix. The maximum in tan δ peak, which corresponds to the glass transition temperature T_g, is often different from the T_g determined with DSC. This difference is explained by the distinctive principles involved in these two techniques (DSC and DMA):DSC measures the change in heat capacity as the chains evolve from the frozen to the unfrozen state, whereas DMA measures the change in mechanical response by these chains. Additionally, we note that a difference in T_g determined by DSC and DMA is observed in the case of semicrystalline polymers and in the present case of an amorphous matrix it is expected to be even larger. The two techniques effectively yield different average values describing the complex dynamics of chain motion. T_g (called also T_α when determined by DMA) of neat PS was found to be around 122°C and it shifted slightly when CNs were added to the composites. However, a more markedly T_g shift (down to 115°C) was observed when a CN:Surfactant weight ratio of 1:2 or 1:3 was used for composites with 3 and 6% CNs load. This observation agrees with DSC data which showed a decrease of T_g as the surfactant content increased.

Furthermore, Fig. 5 shows that the extent of the relaxation process in composites with no surfactant added was reduced when the CNs content was increased (Fig. 5A), whereas it remained roughly constant at low surfactant concentration (e.g., 1:1 CN:surfactant weight ratio for composites containing 3 and 6% of CNs). The magnitude of the relaxation reached a maximum value in the case of composites containing CN-to-Surfactant weight ratio of 1:2 and drops to lower values at higher CN:Surfactant ratios.

It is generally observed that the magnitude of the main relaxation process is reduced in the presence of the dispersed cellulose. It is ascribed to a decrease in the amount of matrix material and therefore the damping properties of the composite, i.e., a decrease in the number of mobile units participating in the relaxation phenomenon. However, new damping mechanisms can be introduced by filler particles [25]. Possible new damping mechanisms include: (i) particle-particle slippage or friction, (ii) particle-polymer motion at the filler interface, and (iii) change in the properties of the polymer by adsorption onto the filler particle.

If significant specific interactions between polymer and filler occur, a layer of polymer surrounding each dispersed particle will be favored; the properties of this layer differ from those of the bulk polymer. Assuming the dispersed phase particles to be rigid, this leads to an immobilized polymer layer which contributes to the effective filler volume fraction in the compound [25]. In light of these remarks, it is clear that dispersed particles/matrix interactions are much higher for the composite films with CN coated with surfactant compared to the ones without surfactant (or with surfactant at low concentrations) when the compatibility between cellulose and the hydrophobic matrix is not sufficient. It is evident that a CN:Surfactant weight ratio around 1:2 is the optimum. At higher concentrations of surfactant, it is expected that the surfactant self-aggregates and probably do not adhere to the cellulose nanoparticle (but rather remain dispersed in the matrix). These aggregates behave like a plasticizer agent and probably interfere with the transfer of load between the matrix and the reinforcing cellulose particles.

CONCLUSIONS

A major challenge in the performance of the targeted cellulose biocomposites is their compatibility with the hydrophobic polymer matrix. The addition of non-ionic surfactant may improve the compatibility but it could have negative impact on the mechanical properties of the ensuing composite. Surfactant appears to enhance the dispersion of CNs within a hydrophobic PS matrix as indicated by optical microscopy. The dispersion of CNs within a hydrophobic polymer matrix appears to correlate well with turbidity measurements.

DSC and DMA analyses provide evidence of the plasticizing effect of surfactant on the composite films, reducing T_g. The optimum concentration of surfactant was determined from turbidity measurements and optical microscopic observations.

Our results are significant in the production of new materials for new or improved thermal and mechanical properties. Therefore, potential applications of the composites include the manufacture of strong lightweight textile nonwovens, super hydrophobic natural materials or production of bioactive filters and lightweight novel barrier materials for protection against chemical and biological agents.

ACKNOWLEDGMENTS

DMA data was obtained in the Hudson Mesoscale Instrumentation facility of the Cornell Center for Materials Research (CCNR) with support from the National Science Foundation Materials Research Science and Engineering Centers (MRSEC) program.

REFERENCES

1. M.A.S. Azizi Samir, F. Alloin, and A. Dufresne, *Biomacromolecules*, **6**, 612 (2005).

2. E. Dujardin, M. Blaseby, and S. Mann, *J. Mater. Chem.*, **13**, 696 (2003).
3. S. Beck-Candanedo, M. Roman, and D.G. Gray, *Biomacromolecules*, **6**, 1048 (2005).
4. M.A.S. Azizi Samir, F. Alloin, J.-Y. Sanchez, N.E.L. Kissi, and A. Dufresne, *Macromolecules*, **37**, 1386 (2004).
5. M.A.S. Azizi Samir, F. Alloin, J.Y. Sanchez, and A. Dufresne, *Polymer*, **45**, 4149 (2004).
6. G. Chauve, L. Heux, R. Arouini, and K. Mazeau, *Biomacromolecules*, **6**, 2025 (2005).
7. V. Favier, G.R. Canova, J.-Y. Cavaille, H. Chanzy, A. Dufresne, and C. Gauthier, *Polym. Adv. Technol.*, **6**, 351 (1995).
8. V. Favier, H. Chanzy, and J.Y. Cavaille, *Macromolecules*, **28**, 6365 (1995).
9. J.F. Ang, *J. Food Sci.*, **56**, 1682 (1991).
10. E.A. Baldwin and B. Wood, *Hortscience*, **41**, 188 (2006).
11. A. Efentakis, S. Koligliati, and A. Vlachou, *Int. J. Pharm.*, **311**, 147 (2006).
12. N. Ljungberg, C. Bonini, F. Bortolussi, C. Boisson, L. Heux, and J.Y. Cavaille, *Biomacromolecules*, **6**, 2732 (2005).
13. L. Vaisman, G. Marom, and H.D. Wagner, *Adv. Funct. Mater.*, **16**, 357 (2006).
14. D. Roy, J.T. Guthrie, and S. Perrier, *Macromolecules*, **38**, 10363 (2005).
15. D. Roy, *Aust. J. Chem.*, **59**, 229 (2006).
16. A. Valadez-Gonzalez, J.M. Cervantes-Uc, R. Olayo, and P.J. Herrera-Franco, *Compos. B*, **30**, 321 (1999).
17. C. Gousse, H. Chanzy, M.L. Cerrada, and E. Fleury, *Polymer*, **45**, 1569 (2004).
18. C. Gousse, H. Chanzy, G. Excoffier, L. Soubeyrand, and E. Fleury, *Polymer*, **43**, 2645 (2002).
19. M. Abdelmouleh, S. Boufi, M.N. Belgacem, A.P. Duarte, A.B. Salah, and A. Gandini, *Int. J. Adhes. Adhes.*, **24**, 43 (2004).
20. P.J. Herrera-Franco and A. Valadez-Gonzalez, *Compos. B*, **36**, 597 (2005).
21. C. Bonini, L. Heux, J.Y. Cavaille, P. Lindner, C. Dewhurst, and P. Terech, *Langmuir*, **18**, 3311 (2002).
22. D. Bondeson and K. Oksman, *Compos. Interface*, **14**, 617 (2007).
23. L. Petersson, I. Kvien, and K. Oksman, *Compos. Sci. Technol.*, **67**, 2535 (2007).
24. P.M. Claesson, M. Kjellin, O.J. Rojas, and C. Stubenrauch, *Phys. Chem. Chem. Phys.*, **47**, 5501 (2006).
25. A. Dufresne, *Compos. Interface*, **10**, 369 (2003).
26. M.N. Angles and A. Dufresne, *Macromolecules*, **33**, 8344 (2000).
27. Y. Lu, L. Weng, and X. Cao, *Macromol. Biosci.*, **5**, 1101 (2005).
28. A.P. Mathew and A. Dufresne, *Biomacromolecules*, **3**, 609 (2002).